

Induction of Micronuclei in Germinating Onion Seed Root Tip Cells Irradiated with High Energy Heavy Ions

Toshihiro TAKATSUJI^{1*}, Hiroki TAKAYANAGI², Kana MORISHITA², Kumie NOJIMA³, Yoshiya FURUSAWA⁴, Yuka NAKAZAWA⁵, Michiko MATSUSE⁵, Sakura AKAMATSU¹, Natsuko HIRANO¹, Natsuko HIRASHIMA¹, Saori HOTOKEZAKA¹, Toyomi IJICHI¹, Chika KAKIMOTO¹, Tomomi KANEMARU¹, Mayumi KOSHITAKE¹, Akiko MORIUCHI¹, Kensuke YAMAMOTO¹ and Isao YOSHIKAWA¹

Onion seedlings/Micronucleus/Heavy ions/Mathematical model/LET.

Effects of high LET charged particles on a perfect *in-vivo* system are an essential theme for the study of the biological effects of radiation. Germinating onion seeds are independent complete organisms and the radiation induced micronuclei in the root chip cells can be examined quantitatively and theoretically. We irradiated with three types of high energy accelerated heavy ions germinating onion seeds using a synchrotron and observed micronuclei in the root tip cells. Micronuclei induction showed characteristic dose responses of an upward convex bell shape and a steep rise near zero doses for all types of the ions. The bell curve dose responses, however, could be explained by a simple mathematical model. A parameter in the model which indicates micronuclei induction frequency and another parameter which indicates induction frequency of lethal damages (or damages delaying cell divisions) per heavy ion track were both proportional to square of the LET. Because we suspected by-stander effect concerning the dose responses rising steeply near zero doses and tapering off for higher doses, we tested acute irradiation to remove time of information transmittance between cells using a single spill (about 0.3 s) of the synchrotron beam. No difference was detected between normal multiple spill irradiations and single spill.

clear as LET.

Most subjects investigated are restricted to reproductive deaths of irradiated cultured mammalian cells and chromosome aberrations of *in vitro* irradiated human peripheral blood lymphocytes. Reports for other subjects are few.^{10–13} Many experiments indicated that the frequency of lethal damage or chromosome aberrations of a cell per primary charged particle crossing the nucleus was proportional to the square of LET,^{14,15} and a few experiments indicated that some effects like eye color mosaic spots of *drosophila* were almost solely dependent on the absorbed doses.¹¹

Ionization is mainly caused by the Coulomb force between secondary electrons of the radiations and orbital electrons of atoms composing tissue. The energy distribution of the secondary electrons is mainly related to the velocity of the primary particles and not related to LET. Therefore, the LET difference itself should not impact the primary physical events. The main cause of the LET dependences is related to the spatial distribution of the primary radiation products. Many chemical reactions are suppressed with high LET because of depletions of the solutes reacting to the primary radiation products.¹⁶ The proportionality to the square of the LET of the induction of chromosome aberrations can

*Corresponding author: Phone: 095-819-2754,

Fax: 095-819-2754,

E-mail: takatsuj@nagasaki-u.ac.jp

¹Faculty of Environmental Studies, Nagasaki University, Nagasaki 852-8521, Japan; ²Graduate School of Science and Technology, Nagasaki University, Nagasaki 852-8521, Japan; ³Ministry of Education, Culture, Sports, Science and Technology, Chiyoda-Ku, Tokyo, 100-8959, Japan;

⁴National Institute of Radiological Sciences, Chiba, 263-8555, Japan;

⁵Graduate School of Biomedical Sciences, Nagasaki University, Nagasaki 852-8523, Japan.

doi:10.1269/jrr.09028

be explained from the intuitive idea that exchange type chromosome aberrations may be generated from the interaction of two DNA damages. These aberrations can explain the reproductive death because cells having chromosome aberrations are thought to cause reproductive death. Models based on sublesion interactions which are represented by the theory of dual radiation action were supported by this idea, though the idea is not wholly accepted. Goodhead *et al.* strongly protested the idea.¹⁵⁾ The interpretation of LET dependence has not yet been established. Recently, unrelated to macroscopic and abstract theories, investigations by computer simulations of molecular level radiation action are being attempted.⁷⁾

The amount of ionization by radiation is approximately proportional to the absorbed dose. Therefore, the effects dependent on the absorbed dose are conceivably dependent on the amount of the primary radiation product.

If the concept of sublesion interactions is true and the actual object corresponding to the sublesion is some radiation induced biological macroscopic complex, it would be difficult to clearly identify the mechanism by means of molecular level investigations because LET dependence is not the result of the difference in primary chemical products. To find the mechanism of LET dependence, we propose examining LET dependent final biological effects and theoretical constructions to explain these effects. To this end, we have examined the induction of micronuclei into root tip cells of irradiated germinating onion seeds, which are known as an excellent biological dosimeter¹⁰⁾ and an independent complete organism different from cultured cells.

MATERIALS AND METHODS

Onion seedlings

Onion (*Allium cepa* L.) seeds of the variety OK Yellow (Takii Seed Co., Kyoto, Japan) were seeded on two sheets of filter paper, (Qualitative Filter Paper No. 2, TOYO ROSHI KAISHA, Tokyo, Japan) laid in a 90 × 20 mm sterilized plastic dish (SH90-20, Asahi Techno Glass Co., Tokyo, Japan) and soaked with distilled water. The seeds were maintained at about 23°C for 48 hours (some fluctuations of the temperature were inevitable because of transportation condition between laboratories). Twenty germinating seedlings were transferred onto the inside back of the plastic covers of 35 × 13 mm sterilized plastic dishes (Nunclon DELTA 153066, Nunc A/S, Roskilde, Denmark). The plastic covers with the seeds were put on the dishes filled with Kim Wipe soaked with distilled water. The seedlings in the covered dishes then were irradiated with heavy ions across the cover.

Irradiation

Neon, Silicon, and Argon ions accelerated by a HIMAC synchrotron at the National Institute of Radiological Sci-

ences—Heavy-ion Medical Accelerator in Chiba (NIRS-HIMAC) at up to 400, 490 and 500 MeV/u respectively were irradiated. The average linear energy transfer (LET) per track was about 31, 55 and 85 keV/μm respectively. The ions were selected because the LET values are appropriately different from each other. The size of the collimation was set to 60 mm × ∞ (width × height).

The LET's were calculated by fitting theoretical Bragg peak curves to the beam monitor values of the ion beams after passing through various absorbers. The absorbed doses were determined from the values of the beam monitors placed upstream using the relationship between the absorbed doses at the sample position and the values of the beam monitors measured in advance. Details of the irradiation system of NIRS-HIMAC were reported by Torikoshi *et al.*¹⁷⁾

- a. Low absorbed dose single spill exposure and multiple spill exposure to seedlings

Each ion spill comes every 3.3 s. The time length of the spill is about 0.3 s. We exposed the seedlings to the low absorbed dose single ion spill (SS) and compared the effects to that of almost same low absorbed dose multiple spill (50–100) exposure (MS). The SS exposure was performed by manipulating a beam switch while watching the output on a beam monitor.

- b. Normal absorbed dose multiple spill exposure to seedlings
Larger than 50 spills exposure.

Micronucleus assay

Irradiated seedlings were cultured at about 23°C for 18 h. The seedlings were fixed, macerated, and stained for 25 minutes with a solution containing acetic dahlia and 1 N HCl at a volume ratio of 7:3. Acetic dahlia was prepared by dissolving a 0.5 g dahlia violet (Wako Pure Chemical Industries, Ltd., Osaka, Japan) into 100 ml of 30 % acetic acid. The seedlings were washed briefly three times with purified water and the remaining water was soaked out on filter paper. About 1 mm of each root tip was placed onto a slide glass, with a drop of 50 % glycerin, slide cover placed, and the tip was squeezed by tapping on the cover glass. The cover glass was sealed with melted paraffin. Micronuclei were scored with a microscope with a magnification of 400×.

RESULTS

Table 1 is a summary of the data. Fig. 1 is the frequency of micronuclei per cell plotted against the absorbed dose. The data fluctuations and data for the three ions overlap each other. However the data of the same absorbed dose show a tendency to line up in increasing order of LET from the bottom at the low absorbed dose region and in the decreasing order at high absorbed dose region. Figure 2 presents the same data plotted against the mean number of heavy ions crossing a nucleus. Figure 3 is the low mean number data of Fig. 2. These figures enable us to compare the effects of the

Table 1. Summary of micronuclei data in root tip cells of germinating onion seeds irradiated with neon, silicon and argon ions. SS: Single spill exposure. MS: Multiple spill exposure. “Ions per nucleus” indicates mean number of the heavy ions crossing a nucleus. Series of experiments are divided with horizontal spaces. Relative variance is variance of the distribution divided by the average. This variance is an index of the dispersion. If the distribution is a Poissonian, the relative variance becomes unity. “ \pm ” which indicates the standard error expected from the experimental distribution.

Radiation	Dose (Gy)	Ions per Nucleus	No. of Cells	No. of Micronuclei					Average per cell	Relative Variance
				0	1	2	3	4		
Control	0.000	0.00	14874	14818	54	2	0	0	$(3.90 \pm 0.53) \times 10^{-3}$	1.065 ± 0.144
Ne	SS	0.051	0.970	6331	6185	127	15	4	0	$(2.67 \pm 0.23) \times 10^{-2}$
		0.034	0.650	6002	5850	128	23	1	0	$(2.95 \pm 0.25) \times 10^{-2}$
	MS	0.052	0.989	3481	3390	85	6	0	0	$(2.79 \pm 0.30) \times 10^{-2}$
		0.032	0.622	6458	6292	143	22	1	0	$(2.94 \pm 0.24) \times 10^{-2}$
		0.050	0.958	1037	1006	30	1	0	0	$(3.09 \pm 0.55) \times 10^{-2}$
		0.100	1.93	1140	1075	63	2	0	0	$(5.88 \pm 0.72) \times 10^{-2}$
		0.300	5.75	1024	870	135	18	1	0	$(1.699 \pm 0.133) \times 10^{-1}$
		0.500	9.58	1031	833	152	41	5	0	$(2.415 \pm 0.168) \times 10^{-1}$
		0.800	15.33	1075	788	221	61	5	0	$(3.330 \pm 0.184) \times 10^{-1}$
		1.200	23.0	1066	762	190	98	13	3	$(4.10 \pm 0.22) \times 10^{-1}$
		0.300	5.75	1192	1048	123	18	2	1	$(1.418 \pm 0.120) \times 10^{-1}$
		0.500	9.58	1336	1084	197	50	5	0	$(2.335 \pm 0.144) \times 10^{-1}$
		1.000	19.2	1126	857	197	54	16	2	$(3.206 \pm 0.193) \times 10^{-1}$
		1.500	28.7	1092	924	103	40	18	5	$(2.45 \pm 0.20) \times 10^{-1}$
		2.000	38.3	949	776	100	51	19	2	$(2.87 \pm 0.22) \times 10^{-1}$
		0.500	9.58	1074	867	159	43	4	1	$(2.430 \pm 0.167) \times 10^{-1}$
		1.000	19.2	1038	840	128	61	9	0	$(2.669 \pm 0.188) \times 10^{-1}$
		1.500	28.7	916	721	114	63	13	3	$(3.29 \pm 0.24) \times 10^{-1}$
Si	SS	0.077	0.827	6601	5664	239	23	0	1	$(4.38 \pm 0.28) \times 10^{-2}$
		0.074	0.795	5495	5224	236	31	4	0	$(5.64 \pm 0.35) \times 10^{-2}$
	MS	0.077	0.829	6132	5803	293	36	0	0	$(5.95 \pm 0.33) \times 10^{-2}$
		0.070	0.757	6190	5889	264	31	6	0	$(5.56 \pm 0.33) \times 10^{-2}$
		0.500	5.39	1262	955	197	80	19	10	$(3.64 \pm 0.21) \times 10^{-1}$
		1.000	10.8	1087	806	155	91	22	13	$(4.19 \pm 0.25) \times 10^{-1}$
		1.500	16.2	945	733	121	50	25	13	$(3.84 \pm 0.28) \times 10^{-1}$
		0.300	3.24	1459	1247	175	36	1	0	$(1.711 \pm 0.116) \times 10^{-1}$
		0.500	5.39	1149	901	181	55	8	4	$(2.881 \pm 0.183) \times 10^{-1}$
		1.000	10.8	1075	840	138	65	23	7	$(3.49 \pm 0.23) \times 10^{-1}$
		1.500	16.2	1005	848	88	46	17	5	$(2.55 \pm 0.21) \times 10^{-1}$
		2.000	21.6	901	817	42	26	11	2	$(1.66 \pm 0.20) \times 10^{-1}$
Ar	SS	0.136	0.952	5306	4662	529	98	16	1	$(1.464 \pm 0.059) \times 10^{-1}$
		0.135	0.939	6487	5701	633	121	29	0	$(1.483 \pm 0.054) \times 10^{-1}$
	MS	0.146	1.02	5303	4753	459	75	15	1	$(1.241 \pm 0.054) \times 10^{-1}$
		0.135	0.945	5835	5150	550	106	28	0	$(1.458 \pm 0.058) \times 10^{-1}$
		0.050	0.349	842	799	36	7	0	0	$(5.94 \pm 0.93) \times 10^{-2}$
		0.100	0.698	900	798	91	11	0	0	$(1.256 \pm 0.122) \times 10^{-1}$
		0.300	2.09	704	593	80	22	8	1	$(2.16 \pm 0.21) \times 10^{-1}$
		0.500	3.49	759	556	143	42	15	3	$(3.74 \pm 0.26) \times 10^{-1}$
		0.500	3.49	915	696	142	58	18	1	$(3.45 \pm 0.23) \times 10^{-1}$
		1.000	6.98	948	804	91	38	13	2	$(2.257 \pm 0.196) \times 10^{-1}$
		1.500	10.5	846	800	18	17	8	2	$(1.052 \pm 0.170) \times 10^{-1}$
		0.300	2.09	1105	911	139	39	7	8	$(2.489 \pm 0.190) \times 10^{-1}$
		0.500	3.49	1112	927	129	42	12	2	$(2.311 \pm 0.175) \times 10^{-1}$
		1.000	6.98	1001	800	102	59	29	10	$(3.52 \pm 0.26) \times 10^{-1}$
		1.500	10.5	833	739	47	30	13	3	$(1.96 \pm 0.22) \times 10^{-1}$
		2.000	14.0	867	827	27	7	4	0	$(7.27 \pm 1.35) \times 10^{-2}$
										2.17 ± 0.40

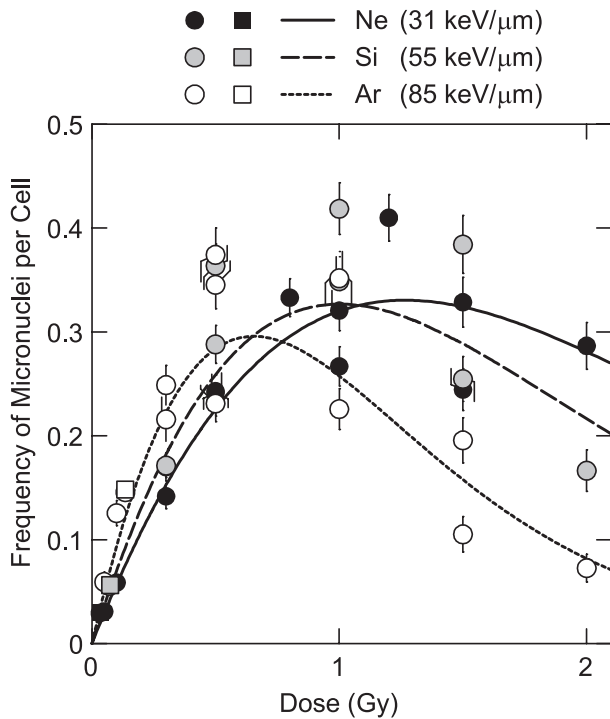


Fig. 1. Frequency of micronuclei per cell plotted against the absorbed dose. Round symbols indicate multiple spill irradiation and square symbols indicate single spill irradiation. Curves represent Eq. (2) with parameters in Table 2.

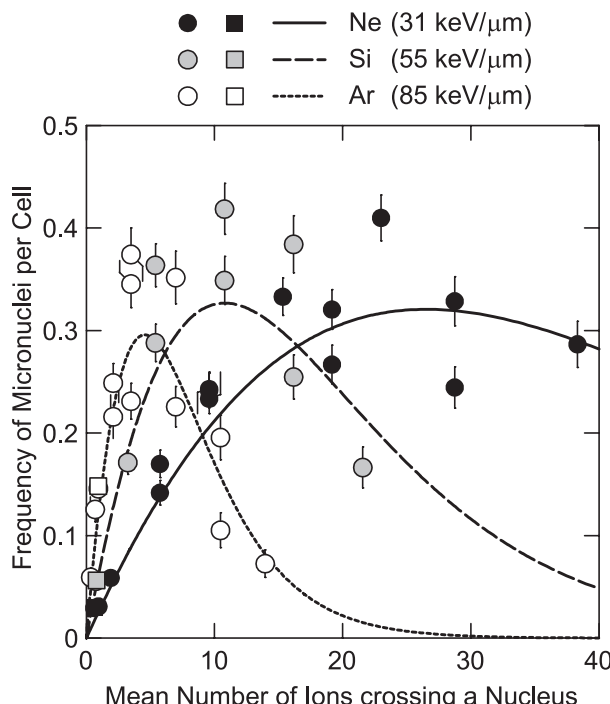


Fig. 2. Frequency of micronuclei per cell plotted against the mean number of ions crossing a cell nucleus. Round symbols indicate multiple spill irradiation and square symbols indicate single spill irradiation. Curves represent Eq. (2) with parameters in Table 2.

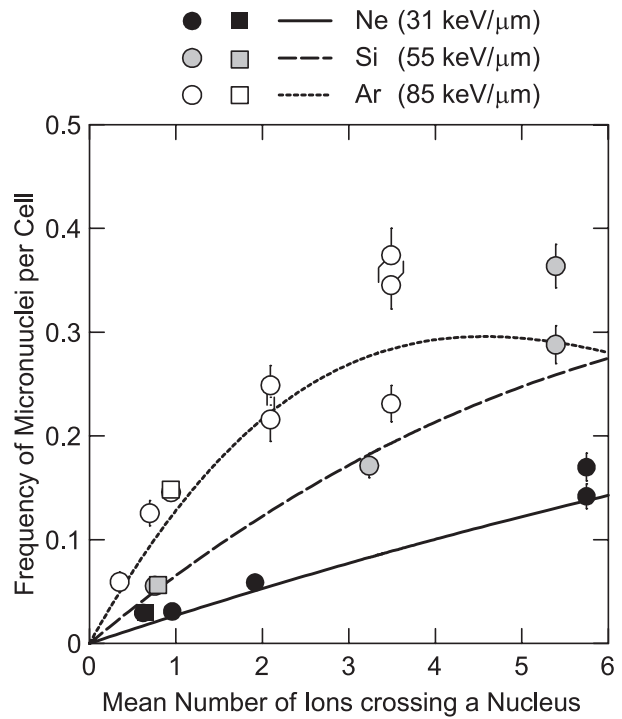


Fig. 3. Low mean number data of Fig. 2.

same numbers of the heavy ions and the difference is clear. The mean number was converted from the absorbed dose using following relationships:

$$\rho D = L\Phi \quad (1)$$

$$m = A\Phi \quad (2)$$

where ρ is tissue density, D is absorbed dose, L is track average LET, Φ is fluence, m is mean number of the particles crossing a nucleus, and A is cross section of the cell nucleus. ρ is assumed 1 g/cm^3 , and A is assumed $95 \mu\text{m}^2$ ($(5.5 \mu\text{m})^2 \times \pi$) because the diameter of nucleus measured by a microscope is about $11 \mu\text{m}$.

Figure 4 is the plot of relative variance (variance divided by mean) of the micronucleus distribution. Figure 5 is the low mean number data of Fig. 4. Relative variance is a factor of a probability distribution which is the most important factor distinguishing the character of intercellular distribution of chromosome aberrations.¹⁸⁾

DISCUSSION

First, we found absorbed dose dependence of the micronucleus induction to steeply rise near zero absorbed doses and gradually becoming gentler with increasing absorbed doses in the low absorbed dose region as seen in Fig. 1. We suspected by-stander effects for the absorbed dose dependence. If some information is transmitted from the irradiated cells to the non irradiated cell nucleus and the information

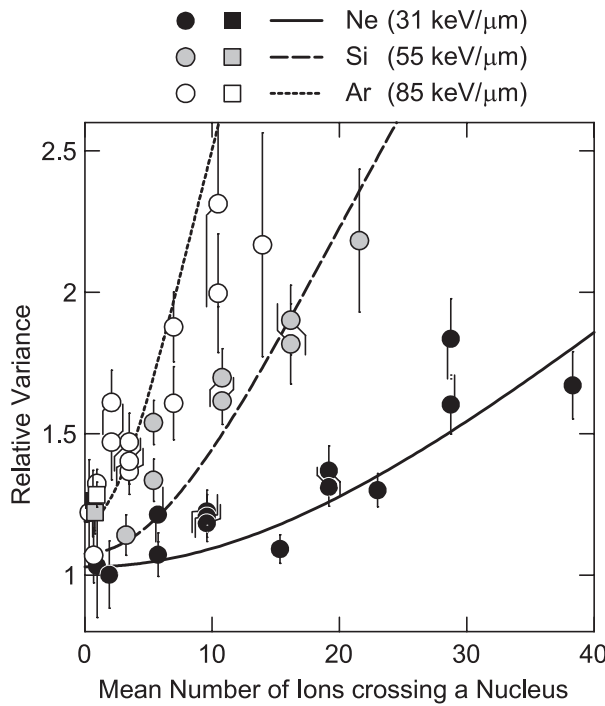


Fig. 4. Relative variance of the intercellular distribution of micronuclei plotted against mean number of ions crossing a cell nucleus. Round symbols indicate multiple spill irradiation and square symbols indicate single spill irradiation. Curves represent Eq. (3) with parameters in Table 2.

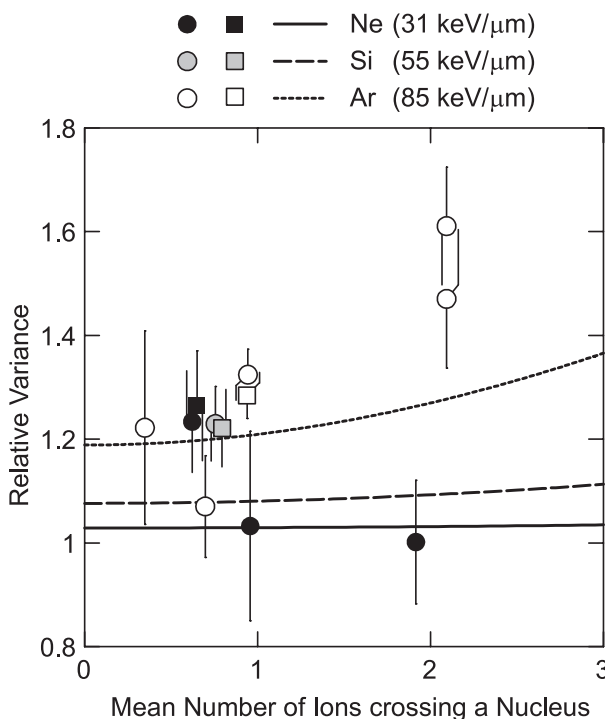


Fig. 5. Low mean number data of Fig. 4.

enhances the radiation effect of the non irradiated cell nucleus when the cell nucleus is irradiated first, larger absorbed dose effects may appear at the low absorbed dose region. Therefore, to detect the time of the information transmittance, we exposed low absorbed doses of the ions for a very short period (0.3 s) using the property of the accelerator and compared the results to the normal prolonged exposures. But no differences were found as seen in Fig. 3 and Fig. 5.

With experiments of higher absorbed doses, we found the bell shaped absorbed dose-effect curve as seen in Fig. 1. The shape of the low absorbed dose region looked like only a part of the bell shape. Therefore, we constructed a theoretical model which can explain the bell shaped radiation dependence. The details are described in the Appendix.

The lines of Fig. 1, Fig. 2 and Fig. 3 are the theoretical curves of the frequency of micronuclei per cell as a function of m (A-16 of Appendix):

$$\mu(m) = \frac{amSe^{-Rm(1-S)}}{1 + e^{-Rm(1-S)}}, \quad (3)$$

where a is the frequency of micronuclei generated in a cell per heavy ion crossing the cell nucleus, S is the surviving rate of a cell hit by a heavy ion and R is the ratio of the cross section of "inactivation target", the region which has a possibility of inactivation with heavy ions crossing, to the nuclear cross section. If some cells are inactivated by heavy ions crossing only the cytoplasm, the optimal value of the inactivation target size would be larger than the nuclear cross section ($R > 1$). For deduction of the equation (3), refer to the deduction of equation (A-16) in the Appendix.

The lines of Fig. 4 and Fig. 5 are theoretical curves of relative variance:

$$\frac{\sigma^2}{\mu} = \frac{a}{2}(mS + 1) - \frac{amSe^{-Rm(1-S)}}{1 + e^{-Rm(1-S)}} + 1 \quad (4)$$

(see (A-19) of appendix).

The values R , S and a in expressions (3) and (4) were obtained minimizing the sum of χ^2 for the experimental data and the theoretical value of μ and $\frac{\sigma^2}{\mu}$ on the condition that R is same for all three ions. The values are summarized in Table 2. The standard errors of the parameters were estimated from the changes of χ^2 when the parameters deviated from the minimum point of χ^2 .

Table 2. R , a and S in Eqs. (3) and (4) fitted to experimental data with minimizing χ^2 . R was determined commonly. a and S were determined for each of the ions.

Kind of Ion (LET)	R		
	Ne (31 keV/μm)	Si (55 keV/μm)	Ar (85 keV/μm)
a	0.0576 ± 0.0015	0.153 ± 0.0057	0.377 ± 0.029
S	0.963 ± 0.012	0.910 ± 0.029	0.788 ± 0.067

The values a and S for different types of heavy ions are plotted against LET as Fig. 6 and 7. The curves of Fig. 6 and Fig. 7 are $a = a_0L^2$ and $S = \exp(-b_0L^2)$ respectively with $a_0 = (5.596 \pm 0.114) \times 10^{-5} \mu\text{m}^2/\text{keV}^2$ and $b_0 = (3.39 \pm 0.67) \times 10^{-5} \mu\text{m}^2/\text{keV}^2$ obtained from regression analyses.

Equations (3) and (4) correctly explain the experiments as

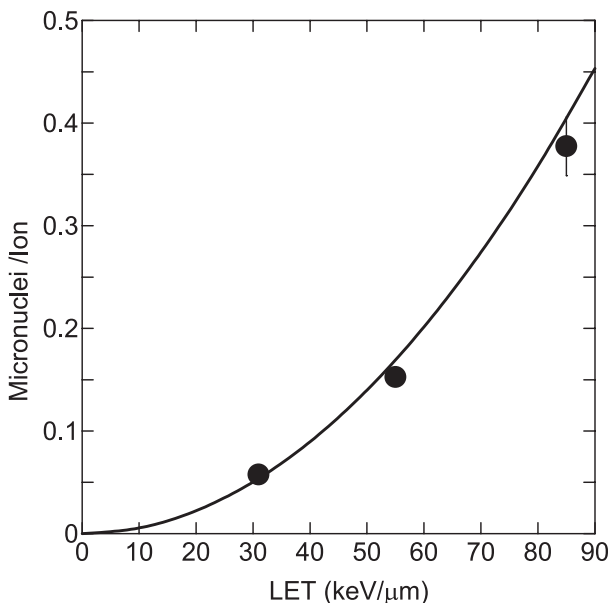


Fig. 6. Induction rate of micronuclei (Value a) of Eq. (3) and (4) fitted to experimental data of Neon, Silicon, and Argon ions plotted against LET.

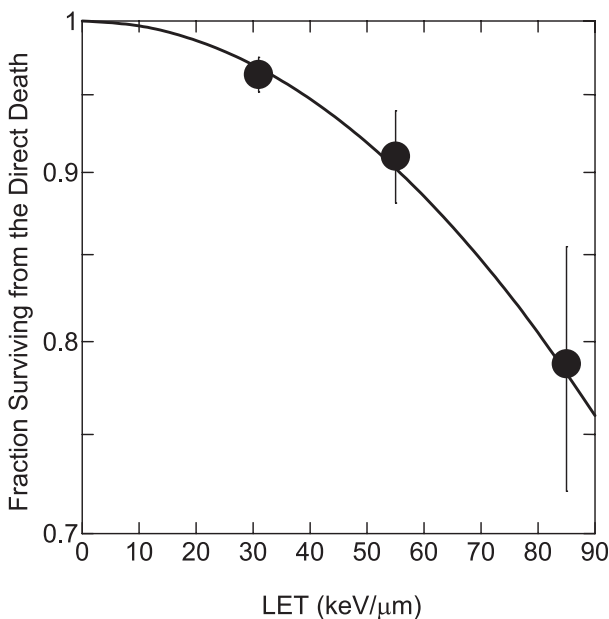


Fig. 7. Fraction surviving from direct death (Value S) of Eq. (3) and (4) fitted to experimental data of Neon, Silicon, and Argon ions plotted against LET.

seen in Fig. 1, Fig. 2 and Fig. 4, and the values a and S follow the equations $a = a_0L^2$ and $S = \exp(-b_0L^2)$ well as seen in Fig. 6 and Fig. 7.

These equations suggest that the frequencies of damage per track of primary charged particle generating micronuclei and cell death are both proportional to the square of the LET. These proportions also agree with the general assumption of sublesion interaction models such as the theory of dual radiation action.^{2,3)}

Cell death and division delay should give the same results within the framework of the model. Onion seedlings are very resistant to radiation. They do not wither with 2–3 Gy of radiation. Therefore most of the lethal damage in the model may very likely be damage by delaying cell divisions. However this is a problem to be solved in the future.

Previous reports for micronuclei induction show dose responses almost linear or slightly bending.^{10,13,19,20)} However, the maximum frequencies of micronuclei are smaller in the previous reports than our report. These previous reports' dose responses are possibly the reason causing the conspicuous bend in the higher absorbed doses. Therefore, it may be possible to apply the mathematical model to these experimental systems.

ACKNOWLEDGEMENTS

This work was supported by the Special Coordination Funds for Research Project with Heavy Ions at the National Institute of Radiological Sciences—Heavy-ion Medical Accelerator in Chiba (NIRS-HIMAC). We greatly appreciate kind guidance of the micronucleus assay using onion seedlings and helpful advice of Dr. Kazuo Fujikawa at Kinki University, Higashi-Osaka City, Japan. We would also like to thank the many students and staff of Nagasaki University who supported our study.

REFERENCES

1. Lea DE (1955) Actions of radiations on living cells, 2nd edition, Cambridge University Press, Cambridge.
2. Kellerer AM and Rossi HH (1972) The theory of dual radiation action. *Cirr Top Radiat Res Q* **8**: 85–158.
3. Kellerer AM and Rossi HH (1978) A generalized formulation of dual radiation action. *Radiat Res* **75**: 471–488.
4. Zaider M and Rossi HH (1980) The synergistic effects of different radiations. *Radiat Res* **83**: 732–739.
5. Suzuki S (1998) A theoretical model for simultaneous mixed irradiation with multiple types of radiation. *J Radiat Res* **39**: 215–221.
6. Suzuki S, *et al* (2002) Models for mixed irradiation with a “reciprocal-time” pattern of the repair function. *J Radiat Res* **43**: 257–267.
7. Yamaguchi H, Ohara H and Waker AJ (2006) A Model for the induction of DNA damages and their evolution into cell clonogenic inactivation. *J Radiat Res* **47**: 197–211.
8. Cucinotta FA, *et al* (2000) Kinetics of DSB rejoining and for-

- mation of simple chromosome exchange aberrations. Int J Radiat Biol **76**: 1463–1474.
9. Savage RK (1998) A brief survey of aberration origin theories. Mutat Res **404**: 139–147.
 10. Fujikawa K, et al (1999) Dose estimation of fast neutrons from a nuclear reactor by micronuclear yields in onion seedlings. J Radiat Res **40 Suppl**: 28–35.
 11. Yoshikawa I, et al (1998) The relative biological effectiveness of accelerated carbon ions with different LET for inducing mitotic crossing over and intragenic reversion of the *white-ivory* allele in *Drosophila* larvae. Int J Radiat Biol **74**: 239–248.
 12. Haag J, Brenot J and Parmentier N (1977) Chromosomal aberrations in pig lymphocytes after neutron irradiation *in vitro*. Radiat Res **70**: 187–197.
 13. Zhang W, et al (2003) Energy-dependent RBE of neutrons to induce micronuclei in root-tip cells of *Allium cepa* onion irradiated as dry dormant seeds and seedlings. J Radiat Res **44**: 171–177.
 14. Takatsuji T, Yoshikawa I and Sasaki MS (1999) Generalized concept of the LET-RBE relationship of radiation-induced chromosome aberration and cell death. J Radiat Res **40**: 59–69.
 15. Goodhead DT, et al (1980) Mutation and inactivation of cultured mammalian cells exposed to beams of accelerated heavy ions, IV. Biophysical interpretation. Int J Radiat Biol **37**: 135–167.
 16. Ohno S, et al (2001) An ion-track structure model based on experimental measurements and its application to calculate radiolysis yields. Radiat Phys Chem **60**: 259–262.
 17. Torikoshi M, et al (2007) Irradiation system for HIMAC. J Radiat Res **48 Suppl**: A15–A25.
 18. Virsk RP and Harder D (1981) Statistical interpretation of the overdispersed distribution of radiation-induced dicentric chromosome aberrations at high LET. Radiat Res **85**: 13–23.
 19. Ban S, et al (1991) Gamma-ray- and fission neutron-induced micronuclei in PHA stimulated and unstimulated human lymphocytes. J Radiat Res **32**: 13–22.
 20. Tanaka K, et al (2000) High incidence of micronuclei in lymphocytes from residents of the area near the Semipalatinsk nuclear explosion test site. J Radiat Res **41**: 45–54.

Received on March 13, 2009
 Revision received on December 16, 2009
 Accepted on February 26, 2010

APPENDIX

Deduction of probability distribution

When k charged particles randomly hit an inactivation target in a cell including the cell nucleus area larger than the nucleus, the probability that l charged particles will hit the cell nucleus in the target follows a binomial distribution;

$$\binom{k}{l} U^l (1-U)^{k-l}, \quad (\text{A-1})$$

where U is the proportion of the nuclear cross section to that of the inactivation target.

Let $p(\lambda, x)$ denote a Poisson distribution of the mean value λ and random variable x . Assuming the probability that x micronuclei are generated in a cell whose nucleus is hit by l particles to be $p(l, x)$ and surviving rate of the cell hit by k charged particles to be S^k ($S \leq 1$), the proportion of cells that live and x micronuclei that are generated irrespective of l is:

$$p_k(x) = S^k \sum_{l=0}^k \binom{k}{l} U^l (1-U)^{k-l} p(l, x). \quad (\text{A-2})$$

When mean number of the particles hitting a nucleus is m , the mean number hitting the inactivation target is Rm ($R = \frac{1}{U}$). Therefore, probability of k hits to the inactivation target is $p(Rm, k)$, and the probability that x micronuclei are generated irrespective of k is

$$p(x) = \sum_{k=0}^{\infty} p(Rm, k) p_k(x). \quad (\text{A-3})$$

Surviving rate of a cell irrespective of k is

$$S_t = \sum_{k=0}^{\infty} p(Rm, k) S^k = e^{-Rm(1-S)}, \quad (\text{A-3})$$

and the rate of killing is

$$K = 1 - S_t = 1 - e^{-Rm(1-S)}. \quad (\text{A-4})$$

Let N denote the total number of cells. The average number of cells surviving and generating x micronuclei is

$$Np(x) = N \sum_{k=0}^{\infty} p(Rm, k) p_k(x). \quad (\text{A-5})$$

The micronuclei become visible after a cell division. If the micronuclei are distributed randomly, the probability that the x_1 micronuclei are distributed to one divided cell and $(x - x_1)$ micronuclei are distributed to another divided cell is a binomial distribution

$$\left(\frac{1}{2}\right)^x \binom{x}{x_1}. \quad (\text{A-6})$$

Because the both divided cells follow the probability, the average number of cells that are divided from cells that have x micronuclei and that have x_1 micronuclei is

$$2Np(x) \left(\frac{1}{2}\right)^x \binom{x}{x_1} \quad (\text{A-7})$$

The average number of cells that have x_1 micronuclei irrespective of x is

$$\begin{aligned}
 F(x_1) &= 2 \sum_{x=x_1}^{\infty} Np(x) \left(\frac{1}{2}\right)^x \binom{x}{x_1} \\
 &= 2N \sum_{x=x_1}^{\infty} \sum_{k=0}^{\infty} p(Rm, k) p_k(x) \left(\frac{1}{2}\right)^x \binom{x}{x_1} \\
 &= 2N \sum_{x=x_1}^{\infty} \sum_{k=0}^{\infty} \frac{R^k m^k}{k!} e^{-Rm} S^k \\
 &\quad \sum_{l=0}^k \frac{k!}{l!(k-l)!} U^l (1-U)^{k-l} \frac{(la)^x}{x!} e^{-la} \left(\frac{1}{2}\right)^x \frac{x!}{x_1!(x-x_1)!} \\
 &= 2N \sum_{x=x_1}^{\infty} \sum_{k=0}^{\infty} R^k m^k e^{-Rm} S^k \sum_{l=0}^k \frac{U^l (1-U)^{k-l}}{l!(k-l)!} \frac{\left(\frac{la}{2}\right)^x}{x_1!(x-x_1)!} e^{-la}. \tag{A-8}
 \end{aligned}$$

Substituting y for $x - x_1$;

$$\begin{aligned}
 F(x_1) &= 2N \sum_{y=0}^{\infty} \sum_{k=0}^{\infty} R^k m^k e^{-Rm} S^k \sum_{l=0}^k \frac{\left(\frac{la}{2}\right)^{x_1}}{x_1!} \frac{U^l (1-U)^{k-l}}{l!(k-l)!} \frac{\left(\frac{la}{2}\right)^y}{y!} e^{-la} \\
 &= 2N \sum_{k=0}^{\infty} R^k m^k e^{-Rm} S^k \sum_{l=0}^k \frac{\left(\frac{la}{2}\right)^{x_1}}{x_1!} \frac{U^l (1-U)^{k-l}}{l!(k-l)!} e^{-la} \sum_{y=0}^{\infty} \frac{\left(\frac{la}{2}\right)^y}{y!} \\
 &= 2N \sum_{k=0}^{\infty} R^k m^k e^{-Rm} S^k \sum_{l=0}^k \frac{\left(\frac{la}{2}\right)^{x_1}}{x_1!} \frac{U^l (1-U)^{k-l}}{l!(k-l)!} e^{-la} e^{\frac{la}{2}} \\
 &= 2N \sum_{k=0}^{\infty} R^k m^k e^{-Rm} S^k \sum_{l=0}^k \frac{\left(\frac{la}{2}\right)^{x_1}}{x_1!} \frac{\left(Ue^{-\frac{a}{2}}\right)^l (1-U)^{k-l}}{l!(k-l)!} \\
 &= 2N \sum_{k=0}^{\infty} \sum_{l=0}^k \frac{\left(Ue^{-\frac{a}{2}}\right)^l (1-U)^{k-l}}{l!(k-l)!} \frac{\left(\frac{la}{2}\right)^{x_1}}{x_1!} (RmS)^k e^{-Rm} \\
 &= 2N \sum_{l=0}^{\infty} \sum_{k=l}^{\infty} \frac{\left(Ue^{-\frac{a}{2}}\right)^l (1-U)^{k-l}}{l!(k-l)!} \frac{\left(\frac{la}{2}\right)^{x_1}}{x_1!} (RmS)^k e^{-Rm} \tag{A-9}
 \end{aligned}$$

Substituting j for $k - l$;

$$\begin{aligned}
 F(x_1) &= 2N \sum_{l=0}^{\infty} \sum_{j=0}^{\infty} \frac{\left(Ue^{-\frac{a}{2}}\right)^l (1-U)^j \left(\frac{la}{2}\right)^{x_1}}{l! j!} (RmS)^{j+l} e^{-Rm} \\
 &= 2N \sum_{l=0}^{\infty} \frac{\left(Ue^{-\frac{a}{2}}\right)^l (RmS)^l \left(\frac{la}{2}\right)^{x_1}}{l!} e^{-Rm} \sum_{j=0}^{\infty} \frac{(1-U)^j (RmS)^j}{j!}
 \end{aligned}$$

$$\begin{aligned}
 &= 2N \sum_{l=0}^{\infty} \frac{\left(mSe^{-\frac{a}{2}}\right)^l \left(\frac{la}{2}\right)^{x_1}}{l!} \frac{e^{-Rm} e^{(1-U)RmS}}{x_1!} \\
 &= 2Ne^{-m(R-(R-1)S)} \sum_{l=0}^{\infty} \frac{\left(mSe^{-\frac{a}{2}}\right)^l \left(\frac{la}{2}\right)^{x_1}}{l!} \frac{x_1!}{x_1!} \\
 &= 2Ne^{-m(R-(R-1)S)} \frac{\left(\frac{a}{2}\right)^{x_1}}{x_1!} \sum_{l=0}^{\infty} \frac{\left(mSe^{-\frac{a}{2}}\right)^l}{l!}. \tag{A-10}
 \end{aligned}$$

Average number of dead cells is

$$NK = N \left(1 - e^{-Rm(1-S)}\right). \tag{A-11}$$

Average total number of live cells is

$$\begin{aligned}
 \sum_{x=0}^{\infty} F(x) &= 2Ne^{-m(R-(R-1)S)} \sum_{x=0}^{\infty} \sum_{l=0}^{\infty} \frac{\left(\frac{al}{2}\right)^x}{x!} \frac{\left(mSe^{-\frac{a}{2}}\right)^l}{l!} \\
 &= 2Ne^{-m(R-(R-1)S)} \sum_{l=0}^{\infty} \frac{e^{\frac{al}{2}}}{l!} \frac{\left(mSe^{-\frac{a}{2}}\right)^l}{l!} \\
 &= 2Ne^{-m(R-(R-1)S)} \sum_{l=0}^{\infty} \frac{\left(mS\right)^l}{l!} \\
 &= 2Ne^{-m(R-(R-1)S)} e^{mS} \\
 &= 2Ne^{-Rm(1-S)}. \tag{A-12}
 \end{aligned}$$

Average total number of living and dead cells from (A-11) and (A-12)

$$\begin{aligned}
 N_A &= N \left(1 - e^{-Rm(1-S)}\right) + 2Ne^{-Rm(1-S)} \\
 &= N \left(1 + e^{-Rm(1-S)}\right). \tag{A-13}
 \end{aligned}$$

The number of cells which have no micronuclei is sum of the number of live cells which have no micronuclei and dead cells, and the proportion is from (A-10) and (A-13),

$$\begin{aligned}
 p_A(0) &= \frac{N \left(1 - e^{-Rm(1-S)}\right) + F(0)}{N \left(1 + e^{-Rm(1-S)}\right)} \\
 &= \frac{N \left(1 - e^{-Rm(1-S)}\right) + 2Ne^{-m(R-(R-1)S)} \sum_{l=0}^{\infty} \frac{\left(mSe^{-\frac{a}{2}}\right)^l}{l!}}{N \left(1 + e^{-Rm(1-S)}\right)} \\
 &= \frac{N \left(1 - e^{-Rm(1-S)}\right) + 2Ne^{-m(R-(R-1)S)} e^{mSe^{-\frac{a}{2}}}}{N \left(1 + e^{-Rm(1-S)}\right)}
 \end{aligned}$$

$$= \frac{1+2e^{-m\left(R-\left(R-1+\frac{a}{2}\right)S\right)}}{1+e^{-Rm(1-S)}} - e^{-Rm(1-S)}. \quad (\text{A-14})$$

The proportion of cells which have x micronuclei of $x \geq 1$ is

$$p_A(x) = \frac{F(x)}{N(1+e^{-Rm(1-S)})} = \frac{2e^{-m(R-(R-1)S)}}{1+e^{-Rm(1-S)}} \frac{\left(\frac{a}{2}\right)^x}{x!} \sum_{l=0}^{\infty} \frac{\left(mSe^{-\frac{a}{2}}\right)^l}{l!} l^x. \quad (\text{A-15})$$

Deduction of average

Average number of the micronuclei per cell, μ , is the mean of the probability distribution $p_A(x)$, and

$$\begin{aligned} \mu &= \sum_{x=1}^{\infty} xp_A(x) \\ &= \sum_{x=1}^{\infty} x \cdot \frac{2e^{-m(R-(R-1)S)}}{1+e^{-Rm(1-S)}} \frac{\left(\frac{a}{2}\right)^x}{x!} \sum_{l=0}^{\infty} \frac{\left(mSe^{-\frac{a}{2}}\right)^l}{l!} l^x \\ &= \frac{2e^{-m(R-(R-1)S)}}{1+e^{-Rm(1-S)}} \sum_{l=0}^{\infty} \frac{\left(mSe^{-\frac{a}{2}}\right)^l}{l!} \frac{al}{2} \sum_{x=1}^{\infty} \frac{\left(\frac{a}{2}\right)^{x-1}}{(x-1)!} \\ &= \frac{2e^{-m(R-(R-1)S)}}{1+e^{-Rm(1-S)}} \sum_{l=0}^{\infty} \frac{\left(mSe^{-\frac{a}{2}}\right)^l}{l!} \frac{al}{2} e^{\frac{al}{2}} \\ &= \frac{2e^{-m(R-(R-1)S)}}{1+e^{-Rm(1-S)}} \frac{a}{2} \sum_{l=1}^{\infty} \frac{(mS)^l}{(l-1)!} \\ &= \frac{amSe^{-m(R-(R-1)S)}}{1+e^{-Rm(1-S)}} \sum_{l=1}^{\infty} \frac{(mS)^{l-1}}{(l-1)!} \\ &= \frac{amSe^{-m(R-(R-1)S)} e^{mS}}{1+e^{-Rm(1-S)}} \\ &= \frac{amSe^{-Rm(1-S)}}{1+e^{-Rm(1-S)}} \end{aligned} \quad (\text{A-16})$$

Deduction of second-order factorial moment

Second-order factorial moment of $p_A(x)$ is

$$\begin{aligned} \mu_{[2]} &= \sum_{x=2}^{\infty} x(x-1)p_A(x) \\ &= \frac{2e^{-m(R-(R-1)S)}}{1+e^{-Rm(1-S)}} \sum_{x=2}^{\infty} \frac{\left(\frac{a}{2}\right)^x}{(x-2)!} \sum_{l=0}^{\infty} \frac{\left(mSe^{-\frac{a}{2}}\right)^l}{l!} l^x \end{aligned}$$

$$\begin{aligned} &= \frac{2e^{-m(R-(R-1)S)}}{1+e^{-Rm(1-S)}} \sum_{l=0}^{\infty} \frac{\left(mSe^{-\frac{a}{2}}\right)^l}{l!} \left(\frac{al}{2}\right)^2 \sum_{x=2}^{\infty} \frac{\left(\frac{al}{2}\right)^{x-2}}{(x-2)!} \\ &= \frac{2e^{-m(R-(R-1)S)}}{1+e^{-Rm(1-S)}} \sum_{l=0}^{\infty} \frac{\left(mSe^{-\frac{a}{2}}\right)^l}{l!} \left(\frac{al}{2}\right)^2 e^{\frac{al}{2}} \\ &= \frac{2e^{-m(R-(R-1)S)}}{1+e^{-Rm(1-S)}} \left(\frac{a}{2}\right)^2 \sum_{l=0}^{\infty} \frac{(mS)^l (l(l-1)+l)}{l!} \\ &= \frac{2e^{-m(R-(R-1)S)}}{1+e^{-Rm(1-S)}} \left(\frac{a}{2}\right)^2 \left((mS)^2 \sum_{l=2}^{\infty} \frac{(mS)^{l-2}}{(l-2)!} + mS \sum_{l=1}^{\infty} \frac{(mS)^{l-1}}{(l-1)!} \right) \\ &= \frac{a^2 e^{-m(R-(R-1)S)} e^{mS}}{2+2e^{-Rm(1-S)}} \left((mS)^2 + mS \right) \\ &= \frac{a^2 e^{-Rm(1-S)}}{2+2e^{-Rm(1-S)}} mS(mS+1) \end{aligned} \quad (\text{A-17})$$

Deduction of relative variance

Variance can be deduced from second-order factorial moment and mean as follows:

$$\begin{aligned} \sigma^2 &= \overline{(x-\mu)^2} \\ &= \overline{x(x-1)-(2\mu-1)x+\mu^2} \\ &= \mu_{[2]} - (2\mu-1)\mu + \mu^2 \\ &= \mu_{[2]} - \mu^2 + \mu. \end{aligned}$$

Therefore from (A-17) and (A-16),

$$\begin{aligned} \sigma^2 &= \frac{a^2 e^{-Rm(1-S)}}{2+2e^{-Rm(1-S)}} mS(mS+1) - \left(\frac{amSe^{-Rm(1-S)}}{1+e^{-Rm(1-S)}} \right)^2 + \frac{amSe^{-Rm(1-S)}}{1+e^{-Rm(1-S)}} \\ &= \frac{a}{2}(mS+1) \frac{amSe^{-Rm(1-S)}}{1+e^{-Rm(1-S)}} - \left(\frac{amSe^{-Rm(1-S)}}{1+e^{-Rm(1-S)}} \right)^2 + \frac{amSe^{-Rm(1-S)}}{1+e^{-Rm(1-S)}} \\ &= \frac{amSe^{-Rm(1-S)}}{1+e^{-Rm(1-S)}} \left(\frac{a}{2}(mS+1) - \frac{amSe^{-Rm(1-S)}}{1+e^{-Rm(1-S)}} + 1 \right). \end{aligned} \quad (\text{A-18})$$

From (A-16)

$$\frac{\sigma^2}{\mu} = \frac{a}{2}(mS+1) - \frac{amSe^{-Rm(1-S)}}{1+e^{-Rm(1-S)}} + 1. \quad (\text{A-19})$$